A peer-reviewed version of this preprint was published in PeerJ on 18 April 2016.

Stepanenko OV, Roginskii DO, Stepanenko OV, Kuznetsova IM, Uversky VN, Turoverov KK. 2016. Structure and stability of recombinant bovine odorant-binding protein: III. Peculiarities of the wild type bOBP unfolding in crowded milieu. PeerJ 4:e1642 https://doi.org/10.7717/peerj.1642

Structure and stability of recombinant bovine odorant-binding protein: III. Peculiarities of the wild type bOBP unfolding in crowded milieu

Olga V Stepanenko, Denis O Roginskii, Olesya V Stepanenko, Irina M Kuznetsova, Vladimir N Uversky, Konstantin K Turoverov

Contrarily to the majority of the members of the lipocalin family, which are stable monomers with the specific OBP fold (a β-barrel consisting of a 8-stranded anti-parallel β-sheet followed by a short α-helical segment, a ninth β-strand, and a disordered C-terminal tail) and a conserved disulfide bond, bovine odorant-binding protein (bOBP) does not have such a disulfide bond and forms a domain-swapped dimer that involves crossing the α-helical region from each monomer over the β-barrel of the other monomer. Furthermore, although natural bOBP isolated from bovine tissues exists as a stable domain-swapped dimer, recombinant bOBP has decreased dimerization potential and therefore exists as a mixture of monomeric and dimeric variants. In this article, we investigated the effect model crowding agents of similar chemical nature but different molecular mass on conformational stability of the recombinant bOBP. These experiments were conducted in order shed light on the potential influence of model crowded environment on the unfolding-refolding equilibrium. To this end, we looked at the influence of PEG-600, PEG-4000, and PEG-12000 in concentrations of 80, 150, and 300 mg/mL on the equilibrium unfolding and refolding transitions induced in the recombinant bOBP by guanidine hydrochloride.

Structure and Stability of Recombinant Bovine Odorant-Binding Protein: III. Peculiarities of the Wild Type bOBP Unfolding in Crowded Milieu

Olga V. Stepanenko,[1] Denis O. Roginskii,[1] Olesya V. Stephanenko,[1] Irina M. Kuznetsova,[1] Vladimir N. Uversky,[1,2,*] and Konstantin K. Turoverov[1,3,*]

[1]Laboratory of structural dynamics, stability and folding of proteins, Institute of Cytology, Russian Academy of Sciences, St. Petersburg, Russia;

[2]Department of Molecular Medicine and USF Health Byrd Alzheimer's Research Institute, Morsani College of Medicine, University of South Florida, Tampa, FL, USA;

[3]Peter the Great St. Petersburg Polytechnic University, St. Petersburg, Russia

***To whom correspondence should be addressed**: VNU, Department of Molecular Medicine, University of South Florida, 12901 Bruce B. Downs Blvd. MDC07, Tampa, Florida 33612, USA, E-mail: vuversky@health.usf.edu; KKT, Institute of Cytology, Russian Academy of Sciences, Tikhoretsky Av., 4, St. Petersburg 194064, Russia, E-mail: kkt@incras.ru

Running title: Unfolding of bOBP in crowded environments

ABSTRACT

Contrarily to the majority of the members of the lipocalin family, which are stable monomers with the specific OBP fold (a β-barrel consisting of a 8-stranded anti-parallel β-sheet followed by a short α-helical segment, a ninth β-strand, and a disordered C-terminal tail) and a conserved disulfide bond, bovine odorant-binding protein (bOBP) does not have such a disulfide bond and forms a domain-swapped dimer that involves crossing the α-helical region from each monomer over the β-barrel of the other monomer. Furthermore, although natural bOBP isolated from bovine tissues exists as a stable domain-swapped dimer, recombinant bOBP has decreased dimerization potential and therefore exists as a mixture of monomeric and dimeric variants. In this article, we investigated the effect model crowding agents of similar chemical nature but different molecular mass on conformational stability of the recombinant bOBP. These experiments were conducted in order shed light on the potential influence of model crowded environment on the unfolding-refolding equilibrium. To this end, we looked at the influence of PEG-600, PEG-4000, and PEG-12000 in concentrations of 80, 150, and 300 mg/mL on the equilibrium unfolding and refolding transitions induced in the recombinant bOBP by guanidine hydrochloride.

Key words: odorant-binding protein; domain swapping; disulfide bond; unfolding-refolding reaction; ligand binding; conformational stability; macromoleclar crowding

INTRODUCTION

Classical odorant binding proteins (OBPs) are intriguing members of the large lipocalin family, which, due to their ability to interact with different odorants (small hydrophobic molecules of various nature and structure that have to travel from air to olfactory receptors in neurones through the aqueous compartment of nasal mucus (Buck & Axel 1991; Pevsner et al. 1988; Pevsner & Snyder 1990; Snyder et al. 1989)), play important but yet not completely understood role in olfaction (Pelosi 1994). Typically, OBPs are monomeric carrier proteins characterized by a specific 3-D fold, known as a prototypic OBP-fold that represents a β-barrel composed by a 8-stranded anti-parallel β-sheet followed by a short α-helical segment, a ninth β-strand and disordered C-terminal tail (Bianchet et al. 1996; Flower et al. 2000). The internal cavity of the OBP β-barrel is the binding site that can interact with the odorant molecules belonging to different chemical classes (Vincent et al. 2004).

Bovine OBP (bOBP) has a unique dimeric structure, which is different from the monomeric OBP fold found in the majority classical OBPs (see Figure 1) (Bianchet et al. 1996). Each protomer in the bOBP dimer forms a β-barrel via interaction with the α-helical region of another protomer by means of the domains swapping mechanism (Bianchet et al. 1996; Tegoni et al. 1996). The domain swapping mechanism, being described for several dimeric and oligomeric proteins, is known to play important structural and functional roles (Bennett et al. 1995; van der Wel 2012). It is believed that the domain swapping causes the increase in the interface area and thereby affects the overall protein stability (Bennett et al. 1994; Liu & Eisenberg 2002). In some cases it has been shown that the formation of the quaternary structure by means of domain swapping was responsible for the appearance of novel functions in corresponding protein monomers, functions, which were not originally present in the monomeric forms of those

proteins (Liu & Eisenberg 2002). Furthermore, early stages of the amyloid fibril formation are believed to be associated with the formation of domain-swapped oligomers (van der Wel 2012).

Our previous studies revealed that there is a noticeable difference between the recombinant bOBP and a natural form of this protein isolated from tissues (Stepanenko et al. 2014b). Here, recombinant bOBP forms a stable native-like conformation with the decreased dimerization potential and therefore exists as a mixture of monomeric and dimeric variants (Stepanenko et al. 2014b). It is likely that the formation of the domain-swapped dimer by the bOBP represents a complex process that requires particular organization of the secondary and tertiary structures of the bOBP monomers. We hypothesized that the recombinant bOBP has perturbed packing of its α-helical region and some β-strands, and that these perturbations in packing of the secondary structure elements might affect the formation of native domain-swapped dimer (Stepanenko et al. 2014b).

Our previous analysis also revealed that the native dimeric form of the recombinant bOBP is formed under the mildly denaturing conditions (i.e., in the presence of 1.5 M guanidine hydrochloride (GdnHCl)) (Stepanenko et al. 2014b). This process requires noticeable reorganization of the bOBP structure and is accompanied by the formation of a stable, more compact intermediate state which is maximally populated at 0.5 M GdnHCl. Cooperative unfolding of the recombinant bOBP is induced by the increase of the GdnHCl concentration above 1.5 M, whereas this protein is completed by ~3M GdnHCl (Stepanenko et al. 2014b). Despite its disturbed fold, the recombinant bOBP is characterized by high conformational stability, which is comparable with that of the native (isolated from tissue) bOBP (Mazzini et al. 2002), pOBP (Staiano et al. 2007; Stepanenko et al. 2008), and other β-rich proteins (Stepanenko et al. 2012; Stepanenko et al. 2013; Stepanenko et al. 2014a). This high conformational stability

89 is indicated by the fact that the recombinant bOBP unfolding is characterized by the half-
90 transition point of > 2 M GdnHCl (Stepanenko et al. 2014b). We have also established that the
91 unfolding of the recombinant bOBP is a completely reversible process, whereas the preceding
92 process of its dimerization is the irreversible event (Stepanenko et al. 2014b).

93

94 One of the open challenges in the fields of protein science is the elucidation of the effects
95 of natural cellular environment on protein structure and function, and on the processes of protein
96 folding, unfolding, and aggregation. This challenge is defined (at least in part) by the so-called
97 macromolecular crowding phenomenon, which originates from a known fact that the living cell
98 contains very high concentrations of biological macromolecules (proteins, nucleic acids,
99 polysaccharides, ribonucleoproteins, etc.), which can range from 80 to 400 mg/mL (Rivas et al.
100 2004; van den Berg et al. 1999; Zimmerman & Trach 1991). This crowded environment is
101 characterized by the restricted amounts of free water (Ellis 2001; Fulton 1982; Minton 1997;
102 Minton 2000b; Zimmerman & Minton 1993; Zimmerman & Trach 1991) and by the limited
103 amount of the space available for a query protein due to the volume occupied by crowders
104 (Minton 2001; Zimmerman & Minton 1993). In fact, it is estimated that the volume occupancy
105 inside the cell is in a range of 5–40% (Ellis & Minton 2003). Therefore, it is expected that in
106 such a crowded milieu, the average spacing between macromolecules should be smaller than the
107 size of the macromolecules themselves (Homouz et al. 2008), and that the macromolecular
108 crowding should have significant effects on various biological processes that depend on the
109 available volume (Minton 2005; Zimmerman & Minton 1993).

110 In the laboratory practice, the potential effects of macromolecular crowding on various
111 biological macromolecules and different biological processes are typically analyzed using

112 solutions containing high concentrations of a model "crowding agent", such as polyethylene
113 glycol (PEG), Dextran, Ficoll, or inert proteins (Chebotareva et al. 2004; Hatters et al. 2002;
114 Kuznetsova et al. 2014; Kuznetsova et al. 2015; Minton 2001). Studies in this field revealed that
115 the efficiency of crowding agents might depend on the ratio between the hydrodynamic
116 dimensions (or occupied volumes) of the crowder and the test molecule, with the most effective
117 conditions being those where the crowder and the test molecule occupy similar volumes (Chen et
118 al. 2011; Minton 1993; Tokuriki et al. 2004). Typically, high concentrations of inert crowders
119 have significant effects on conformational stability and structural properties of some proteins
120 (Christiansen et al. 2010; Engel et al. 2008; Kuznetsova et al. 2014; Mittal & Singh 2013), and
121 may affect various biological processes, such as protein folding, binding of small molecules,
122 enzymatic activity, protein-nucleic acid interactions, protein-protein interactions, protein
123 chaperone activity, pathological protein aggregation, and extent of amyloid formation
124 (Chebotareva et al. 2015a; Chebotareva et al. 2015b; Hatters et al. 2002; Kuznetsova et al. 2014;
125 Kuznetsova et al. 2015; Minton 2000a; Morar et al. 2001; Shtilerman et al. 2002; Uversky et al.
126 2002). For example, we recently conducted a large-scale analysis of the effect of two traditional
127 macromolecular crowders, PEG-8000 and Dextran-70, on the urea-induced unfolding of eleven
128 globular proteins belonging to different structural classes (Stepanenko et al. 2015a). This
129 analysis revealed that crowding agents do not have significant effects on the conformational
130 stability of small, monomeric, positively charged proteins but stabilize oligomeric negatively
131 charged proteins (Stepanenko et al. 2015a). Since different polymers were shown to have very
132 different effects on the conformational stability of a given protein, it has been concluded that the
133 excluded volume effect is not the only factor influencing the protein behavior in the crowded
134 environments, and that the inequality of different crowders in affecting the conformational

stability of proteins can be explained by the ability of the crowding agents to change the solvent properties of aqueous media (Stepanenko et al. 2015a).

In the first article of this series we compared structural and functional properties of the recombinant wild type bOBP and its mutants that cannot dimerize via the domain swapping (Stepanenko et al. 2015b). The analysis revealed that none of the amino acid substitutions introduced to the bOBP affected functional activity of the protein and that the ligand binding leads to the formation of a more compact and stable state of the recombinant bOBP and its mutant monomeric forms (Stepanenko et al. 2015b). Second article of the series was dedicated to the analysis of conformational stabilities of the recombinant bOBP and its monomeric variants in the absence and presence of the natural ligand (Stepanenko et al. 2015c). We showed that the unfolding-refolding pathways of the recombinant bOBP and its monomeric forms are similar and do not depend on the oligomeric status of the protein, suggesting that the information on the unfolding-refolding mechanism is encoded in the structure of the bOBP monomers (Stepanenko et al. 2015c). On the other hand that previous work indicated that the bOBP unfolding process is significantly complicated by the domain-swapped dimer formation, and that the rates of the unfolding-refolding reactions are controlled by the environmental conditions (Stepanenko et al. 2015c).

In this work, we investigated the peculiarities of the unfolding-refolding processes of the recombinant bOBP in the presence of different concentrations of model crowding agents, such as PEGs of different molecular masses. To this end, we looked at the influence of PEG-600, PEG-4000 and PEG-12000 in concentrations of 80, 150, and 300 mg/mL on the conformational stability of the recombinant bOBP against the GdnCl-induced unfolding.

MATHERIAL AND METHODS

Materials

GdnHCl (Nacalai Tesque, Japan), ANS (ammonium salt of 8-anilinonaphtalene-1-sulfonic acid; Fluka, Switzerland) and crowding agents (PEG600, PEG4000 and PEG12000; Sigma-Aldrich, USA) were used without further purification. The protein concentration was 0.1 – 0.2 mg/mL. The experiments were performed in 20 mM Na-phosphate-buffered solution at pH 7.8.

Gene expression and protein purification

The plasmid pT7-7-bOBP which encodes bOBP with a poly-histidine tag were used to transform *Escherichia coli* BL21(DE3) host (Invitrogen) (Stepanenko et al. 2014b). The protein expression was induced by incubating the cells with 0.3 mM of isopropyl-beta-D-1-thiogalactopyranoside (IPTG; Fluka, Switzerland) for 24 h at 37 °C. The recombinant protein was purified with Ni+-agarose packed in HisGraviTrap columns (GE Healthcare, Sweden). The protein purity was determined through SDS-PAGE in 15% polyacrylamide gel (Laemmli 1970).

Fluorescence spectroscopy

Fluorescence experiments were performed using a Cary Eclipse spectrofluorimeter(Varian, Australia) with microcells FLR (10 x 10 mm; Varian, Australia). Fluorescence lifetime were measured using a “home built” spectrofluorimeter with a nanosecond impulse (Stepanenko et al. 2012; Stepanenko et al. 2014b; Turoverov et al. 1998) as well as micro-cells (101.016-QS 5 x 5 mm; Hellma, Germany). Tryptophan fluorescence in the protein was excited at the long-wave absorption spectrum edge (λ_{ex} = 297 nm), wherein the tyrosine residue contribution to the bulk

protein fluorescence is negligible. The fluorescence spectra position and form were characterized using the parameter $A = I_{320}/I_{365}$, wherein I_{320} and I_{365} are the fluorescence intensities at the emission wavelengths 320 and 365 nm, respectively (Turoverov & Kuznetsova 2003). The values for parameter *A* and the fluorescence spectrum were corrected for instrument sensitivity. The tryptophan fluorescence anisotropy was calculated using the equation $r = (I_V^V - GI_H^V)/(I_V^V + 2GI_H^V)$, wherein I_V^V and I_H^V are the vertical and horizontal fluorescence intensity components upon excitement by vertically polarized light. *G* is the relationship between the fluorescence intensity vertical and horizontal components upon excitement by horizontally polarized light $(G = I_V^H / I_H^H)$, λ_{em} = 365 nm (Turoverov et al. 1998). The fluorescence intensity for the fluorescent dye ANS was recorded at λ_{em} = 480 nm (λ_{ex} = 365 nm). Protein unfolding was initiated by manually mixing the protein solution (40 µl) with a buffer solution (510 µl) that included the necessary GdnHCl concentration and crowding agent concentration. The GdnHCl concentration was determined by the refraction coefficient using an Abbe refractometer (LOMO, Russia; (Pace 1986)). The dependences of different fluorescent characteristics bOBP on GdnHCl were recorded following protein incubation in a solution with the appropriate denaturant concentration at 4 ºC for different times (see in the text). The protein refolding was initiated by diluting the pre-denatured protein (in 3.0 M GdnHCl, 40 µl) with the buffer or denaturant solutions at various concentrations (510 µl), containing crowding agent. The spectrofluorimeter was equipped with a thermostat that holds the temperature constant at 23 °C.

Circular dichroism measurements

The CD spectra were generated using a Jasco-810 spectropolarimeter (Jasco, Japan). Far-UV CD spectra were recorded in a 1-mm path length cell from 260 nm to 190 nm with a 0.1 nm step size. Near-UV CD spectra were recorded in a 10-mm path length cell from 320 nm to 250 nm with a 0.1 nm step size. For the spectra, we generated 3 scans on average. The CD spectra for the appropriate buffer solution were recorded and subtracted from the protein spectra.

RESULTS AND DISCUSSION

bOBP unfolding in the presence of PEG-600

Our analysis revealed that in the presence of low concentrations of PEG-600 (80 mg/mL), shapes of the curves describing the GdnHCl-induced unfolding of the recombinant bOBP were similar to the shapes of corresponding curves recorded in the absence of crowder. However, the half-transition points for the unfolding curves measured in the presence of PEG-600 were shifted towards the higher GdnHCl concentrations (see Figure 2A). Table 1 shows that the values of the parameter A and fluorescence anisotropy r measured for the recombinant bOBP in the presence of 80 mg/mL PEG-600 were somewhat higher than the corresponding values measured in the absence of crowder. The increase in the PEG-600 concentration to 150 mg/mL resulted in the more pronounced increase in the parameter A and fluorescence anisotropy r values. Figure 2B shows that when the 150 mg/mL of PEG-600 are added to the solution of the recombinant bOBP, the pre-transition region of the unfolding curve flattens and the transition happens at higher GdnHCl concentrations than the unfolding in the presence of the 80 mg/mL PEG-600.

Curiously, the curves describing the recombinant bOBP refolding from the completely unfolded state and recorded in the presence of 80 or 150 mg/mL of PEG-600 did not coincide

223 with the equilibrium unfolding curves recorded under the similar conditions. However, these
224 refolding curves were close to the curves describing unfolding and refolding of the recombinant
225 bOBP alone (i.e., in the absence of crowding agent; see Figure 2A and 2B).

226 Figure 2C shows that the curves describing equilibrium unfolding and refolding of the
227 recombinant bOBP in the presence of 300 mg/mL PEG-600 coincide and the corresponding
228 transitions gained sigmoidal shape. Furthermore, these transitions happened at significantly
229 higher GdnHCl concentrations, then transitions recorded in the presence of 80 or 150 mg/mL of
230 this crowder (see also Figure 6). Table 1 shows that the parameter *A* and fluorescence anisotropy
231 *r* values determined in solutions containing 300 mg/mL PEG-600 are further increased. Мы так
232 же наблюдали незначительное уменьшение величины времени жизни флуоресценции
233 bOBP при повышении концентрации PEG-600 от 80 до 300 mg/mL (Table 1). We also
234 observed a slight decrease in the fluorescence lifetime of recombinant bOBP with increasing
235 concentration of PEG-600 from 80 to 300 mg/mL (Table 1). These data, together with the
236 observed changes in parameter *A* and fluorescence anisotropy *r* values, testify for some
237 compaction of the protein globule in the presence of the crowding agent, which resulted in
238 shorter distances between the quenching groups of the protein and its tryptophan residues.

239 Interestingly, the ANS fluorescence intensity remained substantially unchanged when this
240 hydrophobic fluorescent dye was added to the protein solution in the presence of denaturant and
241 PEG-600 at all concentrations tested (Figure 2). It is likely that these data reflect the fact that the
242 presence of this crowding agent prevents direct ANS-protein interactions.

243

244 *bOBP unfolding in the presence of PEG-4000 and PEG-12000*

Addition of the increasing concentrations of PEG-4000 and PEG-12000 was accompanied by the increase in the values of the parameter *A* and fluorescence anisotropy *r*, as well as the value of fluorescence lifetime (see Table 1). It is worth noting that the value of fluorescence lifetime for recombinant bOBP in the presence of 80 mg/mL of PEG-4000 was significantly lower that the corresponding value of this parameter measured for bOBP in the presence of 80 mg/mL of PEG-12000, and especially in the presence of 80 mg/mL of PEG-600. However, at increasing the PEG-4000 and PEG-12000 concentration to 300 mg/mL, the value of the fluorescence lifetime of recombinant bOBP increased to the values measured for bOBP in the presence of 300 mg/mL of PEG-600. These data suggest that the crowding agents with different molecular weights have different effects on structure of the protein.

Curiously, when the unfolding-refolding process of the recombinant bOBP was analyzed in the presence of 80 mg/mL of PEG-4000 or PEG-12000, the corresponding transitions curves coincided with each other and with curve describing the equilibrium unfolding-refolding processes in the recombinant bOBP alone (see Figure 3A and 4A). Subsequent increase in concentration of PEG-4000 and PEG-12000 to 150 mg/mL did not change the shape of corresponding curves, but lead to an insignificant and equal for both crowding agents shift of the unfolding transition to higher GdnHCl concentrations (see Figures 3B and 4B). Furthermore, the half-transition point for the bOBP unfolding in the presence of 150 mg/mL of PEG-4000 or PEG-12000 is observed at a significantly lower GdnHCl concentrations than in the presence of 150 mg/mL of PEG-600 (Figure 6).

Figure 3C shows that when PEG-4000 concentration was increased to 300 mg/mL the curve describing the equilibrium unfolding-refolding transitions of bOBP became sigmoidal and coincided with the corresponding curve describing equilibrium unfolding-refolding of this

protein in the presence of 300 mg/mL PEG-600 (see also Figure 6). Although the GdnHCl-induced unfolding curve of the recombinant bOBP in the presence of 300 mg/mL PEG-12000 was also sigmodal (see Figure 4C), the corresponding transition occurred at significantly lower GdnHCl concentrations (Figure 6). The ANS fluorescence intensity in the presence of PEG-4000 or PEG-12000 shows almost no dependence on denaturant concentration (Figure 3 and 4). This provides further support for the crowder-induced interruption of interaction between the ANS molecules and the protein.

Curiously, similar to the results reported in our previous study (Stepanenko et al. 2015c), analysis of the recombinant bOBP unfolding in the presence of various concentrations of different crowders revealed that the GdnHCl dependence of various structural characteristics depends on the incubation time of this protein in the presence of the denaturant (see Figures 2-4). In fact, during the unfolding in crowded milieu, equilibrium values of the analyzed structural characteristics of the recombinant bOBP were reached after the incubation of this protein in the presence of the desired GdnHCl concentration for 72 hrs. This analysis also revealed the presence of noticeable hysteresis between the curves describing the equilibrium unfolding and refolding of bOBP when the corresponding measurements were conducted after incubation of the corresponding solution for 1 hour before the measurements (see Figures 2-4).

Figure 5A shows that the tertiary structure of the recombinant bOBP was not affected by low concentrations (80 mg/mL) of PEG-600, PEG-4000, and PEG-12000. However, although the near-UV CD spectra of this protein measured in the presence of high concentrations of crowding agents soon after mixing (~1h) were different from the corresponding spectrum measured for bOBP alone (see Figure 5B and 5C), this structural difference disappeared after the prolonged incubation of this protein under the corresponding conditions. The secondary structure

of the recombinant bOBP was not changed in the presence of PEG-600, PEG-4000 and PEG-12000, as evidenced by the coincidence of the values of the ellipticity in the far-UV spectrum region recorded for the protein alone or in the presence of all crowding agents at all concentrations tested (Figures 2-4).

The existence of some dependence of the bOBP structure on the time of incubation in the presence of crowders was further supported by the analysis of the intrinsic tryptophan florescence (see bottom panels in Figure 5). Increase in the incubation time of the recombinant bOBP in the presence of 80 or 150 mg/mL of crowding agents generates fluorescence spectra that practically coincide with the spectrum of intrinsic fluorescence of the protein alone. However, when concentration of the crowding agents was increased to 300 mg/mL, the intensity of the tryptophan fluorescence was noticeably enhanced. In fact, the intensities of the fluorescence spectra measured in the presence of high concentrations of PEG-4000 and PEG-12000 were slightly higher, and spectra measured in the presence of 300 mg/mL PEG-600 markedly exceeded the bOBP fluorescence intensity in the solution without crowding agents.

CONCLUSIONS

Our analysis revealed that effects of crowding agents on the structural properties of the recombinant bOBP and on the unfolding-refolding processes of this protein depend on the crowder concentration and size. Being added at low concentrations (80 mg/mL), PEG-600 significantly stabilizes the native sate of the recombinant bOBP but did not influence the mechanism of the unfolding-refolding process. This is evidenced by the mismatch of the transition curves describing the bOBP unfolding and refolding. Low concentrations (80 mg/mL)

313 of PEG-4000 and PEG-12000 possess comparable effects – they do not affect the unfolding-
314 refolding pathway but lead to moderate increase in the stability of recombinant bOBP to
315 denaturing effects of GdnHCl. It is likely that the PEG-4000 and PEG-12000 action can be
316 associated with a slight increase in the solution viscosity in the presence of these agents.

317 Moderate concentrations (150 mg/mL) of crowding agents lead to further increase in the
318 conformational stability of the recombinant bOBP. Under these conditions, PEG-600 possesses
319 more pronounced stabilizing effects than PEG-4000 and PEG-12000 do. At the highest
320 concentrations of crowding agents analyzed in this study (300 mg/mL), their effects on bOBP
321 were somewhat changed. In fact, our data show that even in the absence of denaturant, there is a
322 substantial compaction of a protein globule and a shift of the conformational equilibrium towards
323 the native dimeric form of the bOBP. Furthermore, the bOBP unfolding curves measured in the
324 presence of high concentrations of crowding agents become sigmoidal, suggesting that the
325 unfolding of this protein under such conditions can be described as an all-or-none transition.
326 Curiously, these changes were essentially dependent on the size of crowding agents, with PEG-
327 12000 possessing smallest stabilizing effects.

328 Therefore, the effect of crowding agents on the structure and conformational stability of
329 the recombinant bOBP depends on two factors: (i) Size of the crowder, with the smaller
330 crowding agents being more effective in the stabilization of the bOBP native dimeric state; and
331 (ii) on the concentration of the crowding agents, with the higher crowder concentrations typically
332 possessing stronger stabilizing effects.

333

ACKNOWLEDGEMENTS

This work was supported by a grant from the Russian Science Foundation RSCF № 14-24-00131.

AUTHOR CONTRIBUTIONS

Olga VS, Olesya VS and DOR collected and analyzed data, contributed to discussion, and wrote the manuscript. Olga VS, IMK, and KKT conceived the idea, supervised the project, contributed to discussion, and reviewed/edited manuscript. VNU analyzed data, contributed to discussion, and wrote the manuscript.

DISCLOSURE

None declared.

REFENCES

Bennett MJ, Choe S, and Eisenberg D. 1994. Domain swapping: entangling alliances between proteins. *Proc Natl Acad Sci U S A* 91:3127-3131.

Bennett MJ, Schlunegger MP, and Eisenberg D. 1995. 3D domain swapping: a mechanism for oligomer assembly. *Protein Sci* 4:2455-2468.

Bianchet MA, Bains G, Pelosi P, Pevsner J, Snyder SH, Monaco HL, and Amzel LM. 1996. The three-dimensional structure of bovine odorant binding protein and its mechanism of odor recognition. *Nat Struct Biol* 3:934-939.

Buck L, and Axel R. 1991. A novel multigene family may encode odorant receptors: a molecular basis for odor recognition. *Cell* 65:175-187.

Chebotareva NA, Eronina TB, Sluchanko NN, and Kurganov BI. 2015a. Effect of Ca2+ and Mg2+ ions on oligomeric state and chaperone-like activity of alphaB-crystallin in crowded media. *Int J Biol Macromol* 76:86-93.

Chebotareva NA, Filippov DO, and Kurganov BI. 2015b. Effect of crowding on several stages of protein aggregation in test systems in the presence of alpha-crystallin. *Int J Biol Macromol* 80:358-365.

Chebotareva NA, Kurganov BI, and Livanova NB. 2004. Biochemical effects of molecular crowding. *Biochemistry (Mosc)* 69:1239-1251.

Chen C, Loe F, Blocki A, Peng Y, and Raghunath M. 2011. Applying macromolecular crowding to enhance extracellular matrix deposition and its remodeling in vitro for tissue engineering and cell-based therapies. *Adv Drug Deliv Rev* 63:277-290.

Christiansen A, Wang Q, Samiotakis A, Cheung MS, and Wittung-Stafshede P. 2010. Factors defining effects of macromolecular crowding on protein stability: an in vitro/in silico case study using cytochrome c. *Biochemistry* 49:6519-6530.

Dutta S, Burkhardt K, Young J, Swaminathan GJ, Matsuura T, Henrick K, Nakamura H, and Berman HM. 2009. Data deposition and annotation at the worldwide protein data bank. *Mol Biotechnol* 42:1-13.

Ellis RJ. 2001. Macromolecular crowding: obvious but underappreciated. *Trends Biochem Sci* 26:597--604.

Ellis RJ, and Minton AP. 2003. Cell biology: join the crowd. *Nature* 425:27-28.

Engel R, Westphal AH, Huberts DH, Nabuurs SM, Lindhoud S, Visser AJ, and van Mierlo CP. 2008. Macromolecular crowding compacts unfolded apoflavodoxin and causes severe aggregation of the off-pathway intermediate during apoflavodoxin folding. *J Biol Chem* 283:27383-27394.

Flower DR, North AC, and Sansom CE. 2000. The lipocalin protein family: structural and sequence overview. *Biochim Biophys Acta* 1482:9-24.

Fulton AB. 1982. How crowded is the cytoplasm? *Cell* 30:345--347.

Hatters DM, Minton AP, and Howlett GJ. 2002. Macromolecular crowding accelerates amyloid formation by human apolipoprotein C-II. *J Biol Chem* 277:7824--7830.

Homouz D, Perham M, Samiotakis A, Cheung MS, and Wittung-Stafshede P. 2008. Crowded, cell-like environment induces shape changes in aspherical protein. *Proc Natl Acad Sci U S A* 105:11754-11759.

Hsin J, Arkhipov A, Yin Y, Stone JE, and Schulten K. 2008. Using VMD: an introductory tutorial. *Curr Protoc Bioinformatics* Chapter 5:Unit 5 7.

Kuznetsova IM, Turoverov KK, and Uversky VN. 2014. What macromolecular crowding can do to a protein. *Int J Mol Sci* 15:23090-23140.

Kuznetsova IM, Zaslavsky BY, Breydo L, Turoverov KK, and Uversky VN. 2015. Beyond the excluded volume effects: mechanistic complexity of the crowded milieu. *Molecules* 20:1377-1409.

Laemmli UK. 1970. Cleavage of structural proteins during the assembly of the head of bacteriophage T4. *Nature* 227:680-685.

Liu Y, and Eisenberg D. 2002. 3D domain swapping: as domains continue to swap. *Protein Sci* 11:1285-1299.

Mazzini A, Maia A, Parisi M, Sorbi RT, Ramoni R, Grolli S, and Favilla R. 2002. Reversible unfolding of bovine odorant binding protein induced by guanidinium hydrochloride at neutral pH. *Biochim Biophys Acta* 1599:90-101.

Merritt EA, and Bacon DJ. 1977. Raster3D: Photorealistic molecular graphics. . *Methods enzymol* 277:505-524.

Minton AP. 1993. Macromolecular crowding and molecular recognition. *J Mol Recognit* 6:211-214.

Minton AP. 1997. Influence of excluded volume upon macromolecular structure and associations in 'crowded' media. *Curr Opin Biotechnol* 8:65--69.

410 Minton AP. 2000a. Implications of macromolecular crowding for protein assembly. *Curr Opin*
411 *Struct Biol* 10:34--39.
412 Minton AP. 2000b. Protein folding: Thickening the broth. *Curr Biol* 10:R97--99.
413 Minton AP. 2001. The influence of macromolecular crowding and macromolecular confinement
414 on biochemical reactions in physiological media. *J Biol Chem* 276:10577--10580.
415 Minton AP. 2005. Models for excluded volume interaction between an unfolded protein and
416 rigid macromolecular cosolutes: macromolecular crowding and protein stability revisited.
417 *Biophys J* 88:971-985.
418 Mittal S, and Singh LR. 2013. Denatured state structural property determines protein
419 stabilization by macromolecular crowding: a thermodynamic and structural approach.
420 *Plos One* 8:e78936.
421 Morar AS, Olteanu A, Young GB, and Pielak GJ. 2001. Solvent-induced collapse of alpha-
422 synuclein and acid-denatured cytochrome c. *Protein Sci* 10:2195--2199.
423 Pace CN. 1986. Determination and analysis of urea and guanidine hydrochloride denaturation
424 curves. *Methods Enzymol* 131:266-280.
425 Pelosi P. 1994. Odorant-binding proteins. *Crit Rev Biochem Mol Biol* 29:199-228.
426 Pevsner J, Hwang PM, Sklar PB, Venable JC, and Snyder SH. 1988. Odorant-binding protein
427 and its mRNA are localized to lateral nasal gland implying a carrier function. *Proc Natl*
428 *Acad Sci U S A* 85:2383-2387.
429 Pevsner J, and Snyder SH. 1990. Odorant-binding protein: odorant transport function in the
430 vertebrate nasal epithelium. *Chem Senses* 15:217-222.
431 Rivas G, Ferrone F, and Herzfeld J. 2004. Life in a crowded world. *EMBO Rep* 5:23-27.
432 Shtilerman MD, Ding TT, and Lansbury PT, Jr. 2002. Molecular crowding accelerates
433 fibrillization of alpha-synuclein: could an increase in the cytoplasmic protein
434 concentration induce Parkinson's disease? *Biochemistry* 41:3855--3860.
435 Snyder SH, Sklar PB, Hwang PM, and Pevsner J. 1989. Molecular mechanisms of olfaction.
436 *Trends Neurosci* 12:35-38.
437 Staiano M, D'Auria S, Varriale A, Rossi M, Marabotti A, Fini C, Stepanenko OV, Kuznetsova
438 IM, and Turoverov KK. 2007. Stability and dynamics of the porcine odorant-binding
439 protein. *Biochemistry* 46:11120-11127.
440 Stepanenko OV, Marabotti A, Kuznetsova IM, Turoverov KK, Fini C, Varriale A, Staiano M,
441 Rossi M, and D'Auria S. 2008. Hydrophobic interactions and ionic networks play an
442 important role in thermal stability and denaturation mechanism of the porcine odorant-
443 binding protein. *Proteins* 71:35-44.
444 Stepanenko OV, Povarova OI, Sulatskaya AI, Ferreira LA, Zaslavsky BY, Kuznetsova IM,
445 Turioverov KK, and Uversky VN. 2015a. Protein unfolding in crowded milieu: What
446 crowding can do to a protein undergoing unfolding? *J Biomol Struct Dyn*:1-0.
447 Stepanenko OV, Roginskii DO, Stephanenko OV, Kuznetsova IM, Uversky VN, and Turoverov
448 KK. 2015b. Structure and stability of recombinant bovine odorant-binding protein: I.
449 Design and analysis of monomeric mutants. . *PeerJ*.
450 Stepanenko OV, Roginskii DO, Stephanenko OV, Kuznetsova IM, Uversky VN, and Turoverov
451 KK. 2015c. Structure and stability of recombinant bovine odorant-binding protein: II.
452 Unfolding of the monomeric forms. . *PeerJ*.
453 Stepanenko OV, Stepanenko OV, Kuznetsova IM, Shcherbakova DM, Verkhusha VV, and
454 Turoverov KK. 2012. Distinct effects of guanidine thiocyanate on the structure of
455 superfolder GFP. *PLoS One* 7:e48809.

456 Stepanenko OV, Stepanenko OV, Kuznetsova IM, Verkhusha VV, and Turoverov KK. 2013.
457 Beta-barrel scaffold of fluorescent proteins: folding, stability and role in chromophore
458 formation. *Int Rev Cell Mol Biol* 302:221-278.
459 Stepanenko OV, Stepanenko OV, Kuznetsova IM, Verkhusha VV, and Turoverov KK. 2014a.
460 Sensitivity of superfolder GFP to ionic agents. *PLoS One* 9:e110750.
461 Stepanenko OV, Stepanenko OV, Staiano M, Kuznetsova IM, Turoverov KK, and D'Auria S.
462 2014b. The quaternary structure of the recombinant bovine odorant-binding protein is
463 modulated by chemical denaturants. *PLoS One* 9:e85169.
464 Tegoni M, Ramoni R, Bignetti E, Spinelli S, and Cambillau C. 1996. Domain swapping creates a
465 third putative combining site in bovine odorant binding protein dimer. *Nat Struct Biol*
466 3:863-867.
467 Tokuriki N, Kinjo M, Negi S, Hoshino M, Goto Y, Urabe I, and Yomo T. 2004. Protein folding
468 by the effects of macromolecular crowding. *Protein Sci* 13:125-133.
469 Turoverov KK, Biktashev AG, Dorofeiuk AV, and Kuznetsova IM. 1998. [A complex of
470 apparatus and programs for the measurement of spectral, polarization and kinetic
471 characteristics of fluorescence in solution]. *Tsitologiia* 40:806-817.
472 Turoverov KK, and Kuznetsova IM. 2003. Intrinsic fluorescence of actin. *J Fluorescence* 13:41-
473 57.
474 Uversky VN, Cooper EM, Bower KS, Li J, and Fink AL. 2002. Accelerated alpha-synuclein
475 fibrillation in crowded milieu. *FEBS Lett* 515:99--103.
476 van den Berg B, Ellis RJ, and Dobson CM. 1999. Effects of macromolecular crowding on
477 protein folding and aggregation. *EMBO J* 18:6927-6933.
478 van der Wel PC. 2012. Domain swapping and amyloid fibril conformation. *Prion* 6:211-216.
479 Vincent F, Ramoni R, Spinelli S, Grolli S, Tegoni M, and Cambillau C. 2004. Crystal structures
480 of bovine odorant-binding protein in complex with odorant molecules. *Eur J Biochem*
481 271:3832-3842.
482 Zimmerman SB, and Minton AP. 1993. Macromolecular crowding: biochemical, biophysical,
483 and physiological consequences. *Annu Rev Biophys Biomol Struct* 22:27--65.
484 Zimmerman SB, and Trach SO. 1991. Estimation of macromolecule concentrations and excluded
485 volume effects for the cytoplasm of Escherichia coli. *J Mol Biol* 222:599--620.

FIGURE LEGENDS

Figure 1. 3-D structure of bOBP. The individual subunits in the protein are in gray and pink. The tryptophan residues in the different subunits are indicated in blue and red as van der Waals spheres. The drawing was generated based on the 1OBP file (Tegoni et al. 1996) from PDB (Dutta et al. 2009) using the graphic software VMD (Hsin et al. 2008) and Raster3D (Merritt & Bacon 1977).

Figure 2. GdnHCl-induced unfolding – refolding of the recombinant bOBP alone (red circles; the data are from (Stepanenko et al. 2014b)) and in the presence of a crowding agent PEG-600 (squares) at low (80 mg/mL, *A*), medium (150 mg/mL, *B*) and high concentration (300 mg/mL, *C*). The protein conformational changes were followed by changes in the parameter *A* (λ_{ex}=297 nm), fluorescence anisotropy *r* at the emission wavelength 365 nm (λ_{ex}=297 nm), the ellipticity at 222 nm and the ANS fluorescence intensity at λ_{em}=480 nm (λ_{ex}=365 nm). Protein was incubated in a solution with the appropriate the appropriate GdnHCl concentration at 4ºC for 1 h (gray squares), 24 h (red circles), 96 h (green squares) and 7 days (dark yellow squares). The open symbols indicate unfolding, whereas the closed symbols represent refolding.

Figure 3. GdnHCl-induced unfolding – refolding of the recombinant bOBP alone (red circles; the data are from (Stepanenko et al. 2014b)) and in the presence of PEG-4000 (squares) at low (80 mg/L *A*), medium (150 mg/mL, *B*) and high (300 mg/L *C*)

509 **concentration.** The protein conformational changes were followed by the changes in the
510 parameter *A* (λ_{ex}=297 nm), fluorescence anisotropy *r* at the emission wavelength 365 nm
511 (λ_{ex}=297 nm), the ellipticity at 222 nm and the ANS fluorescence intensity at λ_{em}=480 nm
512 (λ_{ex}=365 nm). Protein was incubated in a solution with the appropriate GdnHCl concentration at
513 4ºC for 1 h (gray squares), 24 h (light green squares and red circles) and 72 h (green squares).
514 The open symbols indicate unfolding, whereas the closed symbols represent refolding.

515

516 **Figure 4. GdnHCl-induced unfolding – refolding of the recombinant bOBP alone (red**
517 **circles; the data are from (Stepanenko et al. 2014b)) and in the presence of PEG-12000**
518 **(squares) at low (80 mg/mL, *A*), medium (150 mg/mL, *B*) and high concentrations (300**
519 **mg/mL, *C*).** The protein conformational changes were followed by changes in the parameter *A*
520 (λ_{ex}=297 nm), fluorescence anisotropy *r* at the emission wavelength 365 nm (λ_{ex}=297 nm), the
521 ellipticity at 222 nm, and the ANS fluorescence intensity at λ_{em}=480 nm (λ_{ex}=365 nm). Protein
522 was incubated in a solution with the appropriate GdnHCl concentration at 4ºC for 1 h (gray
523 squares), 24 h (light green squares and red circles) and 72 h (green squares). The open symbols
524 indicate unfolding, whereas the closed symbols represent refolding.

525

526 **Figure 5. Changes in the near-UV CD spectra (upper panels) and the tryptophan**
527 **fluorescence spectra (bottom panels) of bOBP alone (black lines) and in the presence of**
528 **PEG-600 (green colors), PEG-4000 (red colors) and PEG-12000 (blue colors).** The
529 measurements were preceded by incubating the protein in a solution with crowding agent at 4ºC
530 for 1 h (PEG-600 – light-green, PEG-4000 – pink, PEG-12000 – light blue) and 72 – 96 h (PEG-

531 600 – green, PEG4-000 – red, PEG-12000 –blue). The concentrations of crowding agents were
532 80 mg/mL (***A***), 150 mg/mL (***B***) and 300 mg/mL (***C***).

533

534 **Figure 6. GdnHCl-induced unfolding – refolding of the recombinant bOBP alone (gray**
535 **circles; the data are from (Stepanenko et al. 2014b)) and in the presence of crowding agents**
536 **PEG-600 (green colors), PEG-4000 (red colors) and PEG-12000 (blue colors).** The protein
537 conformational changes were followed by the changes in parameter *A* and fluorescence
538 anisotropy at the emission wavelength 365 nm (λ_{ex}=297 nm). The measurements were preceded
539 by incubating the protein in a solution with the appropriate GdnHCl concentration at 4ºC for 72 –
540 96 h. The open symbols indicate unfolding, whereas the closed symbols represent refolding.
541 Applied concentrations of crowding agents were 80 mg/mL (***A***; squares, PEG-600 – light green,
542 PEG-4000 – pink, PEG-12000 – light blue), were 150 mg/mL (***B***; circles, PEG-600 – green,
543 PEG-4000 – red, PEG-12000 –blue) and were 300 mg/mL (***C***; triangles, PEG-600 – dark yellow,
544 PEG-4000 – brown, PEG-12000 – dark blue). ***D*** panel represents all intrinsic fluorescence data
545 for comparison purpose.

Table 1(on next page)

Characteristics of intrinsic fluorescence of recombinant bOBP alone and in the different crowding agents.

Table 1. Characteristics of intrinsic fluorescence of recombinant bOBP alone and in the different crowding agents.

	λ_{max}, nm (λ_{ex}=297 nm)	Parameter *A* (λ_{ex}=297 nm)	*r* (λ_{ex}=297 nm, λ_{em}=365 nm)	τ, nm (λ_{ex}=297 nm, λ_{em}=335 nm)
bOBPwt in buffered solution*	335	1.21	0.170	4.37 ± 0.19
bOBPwt/PEG-600 80 mg/ml	333	1.35	0.191	4.40 ± 0.17
bOBPwt/PEG-600 150 mg/ml	332	1.40	0.195	4.09 ± 0.03
bOBPwt/PEG-600 300 mg/ml	334	1.43	0.196	4.22 ± 0.03
bOBPwt/PEG-4000 80 mg/ml	334	1.29	0.194	3.68 ± 0.25
bOBPwt/PEG-4000 150 mg/ml	334	1.31	0.197	3.94 ± 0.10
bOBPwt/PEG-4000 300 mg/ml	335	1.37	0.20	4.19 ± 0.10
bOBPwt/PEG-12000 80 mg/ml	335	1.28	0.192	3.96 ± 0.04
bOBPwt/PEG-12000 150 mg/ml	335	1.32	0.203	4.16 ± 0.07
bOBPwt/PEG-12000 300 mg/ml	335	1.40	0.203	4.20 ± 0.50

* The data are from (Stepanenko et al. 2014b)

1

3-D structure of bOBP.

Figure 1. 3-D structure of bOBP. The individual subunits in the protein are in gray and pink. The tryptophan residues in the different subunits are indicated in blue and red as van der Waals spheres. The drawing was generated based on the 1OBP file (Tegoni et al. 1996) from PDB (Dutta et al. 2009) using the graphic software VMD (Hsin et al. 2008) and Raster3D (Merritt & Bacon 1977).

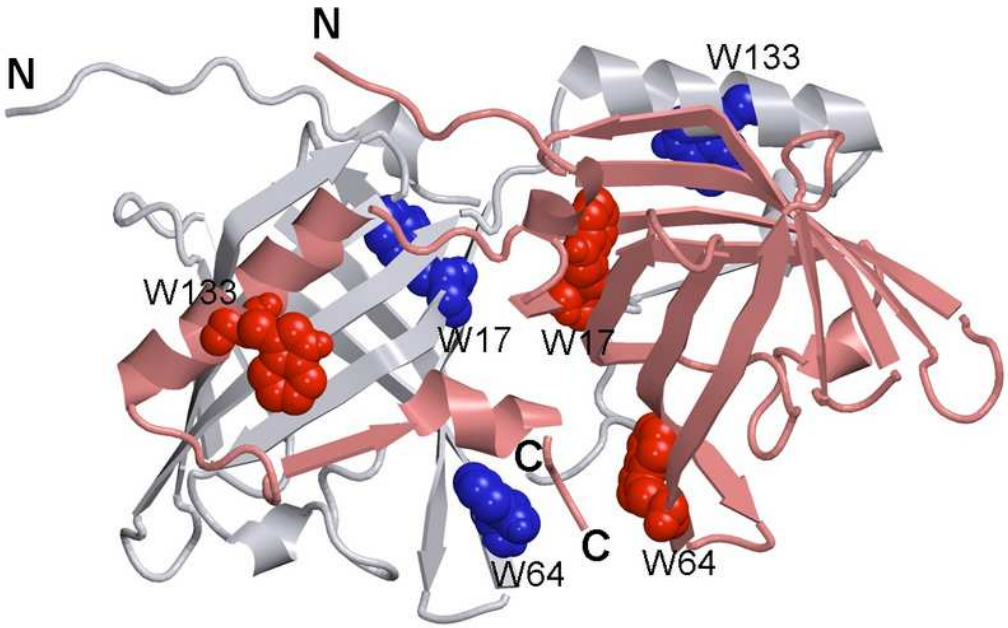

2

GdnHCl-induced unfolding – refolding of the recombinant bOBP alone and in the presence of PEG-600.

Figure 2. GdnHCl-induced unfolding – refolding of the recombinant bOBP alone (red circles; the data are from (Stepanenko et al. 2014b)) and in the presence of a crowding agent PEG-600 (squares) at low (80 mg/mL, *A*), medium (150 mg/mL, *B*) and high concentration (300 mg/mL, *C*). The protein conformational changes were followed by changes in the parameter *A* (λ_{ex}=297 nm), fluorescence anisotropy *r* at the emission wavelength 365 nm (λ_{ex}=297 nm), the ellipticity at 222 nm and the ANS fluorescence intensity at l_{em}=480 nm (l_{ex}=365 nm). Protein was incubated in a solution with the appropriate the appropriate GdnHCl concentration at 4ºC for 1 h (gray squares), 24 h (red circles), 96 h (green squares) and 7 days (dark yellow squares). The open symbols indicate unfolding, whereas the closed symbols represent refolding.

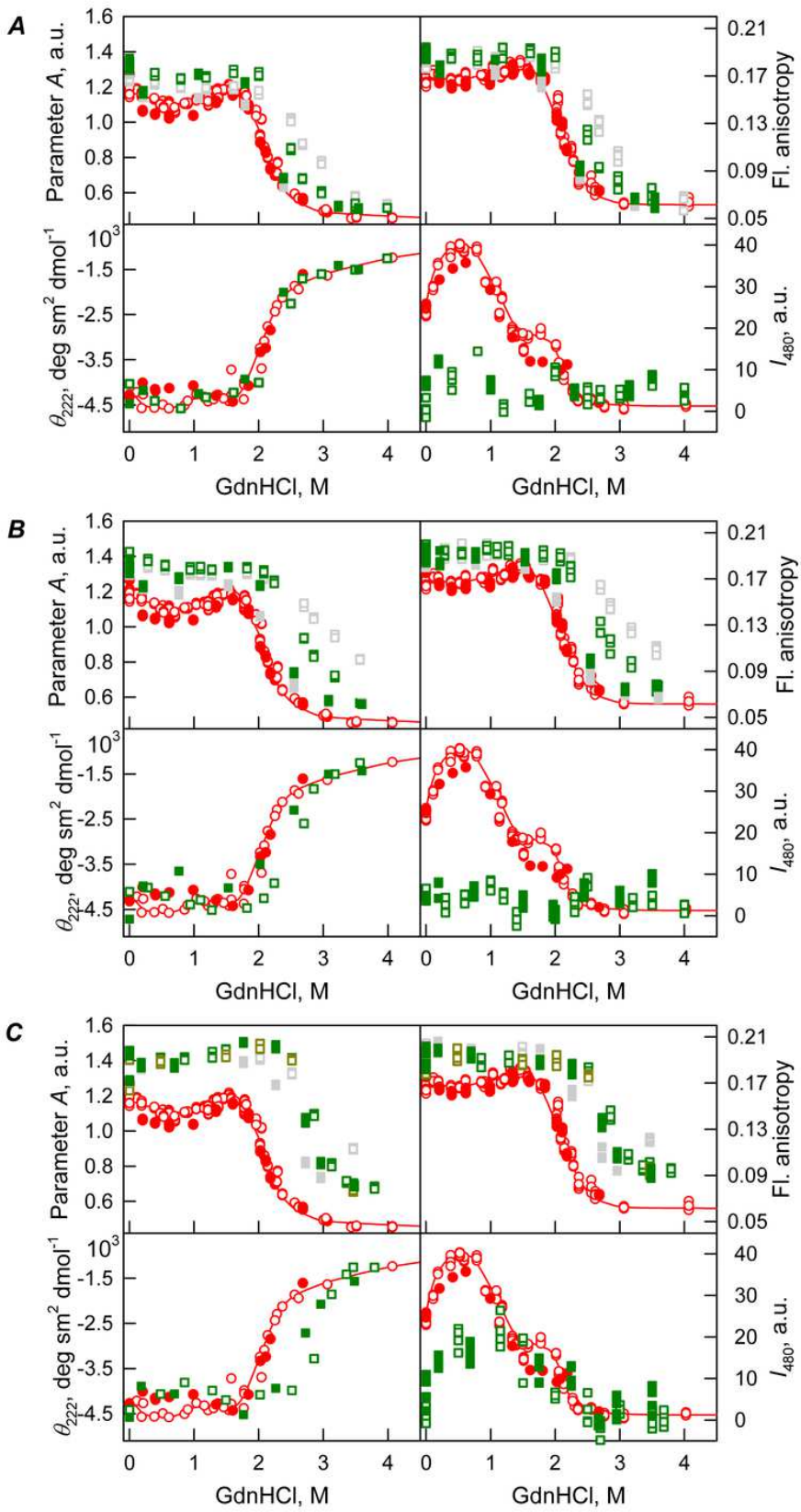

3

GdnHCl-induced unfolding – refolding of the recombinant bOBP alone and in the presence of PEG-4000.

Figure 3. GdnHCl-induced unfolding – refolding of the recombinant bOBP alone (red circles; the data are from (Stepanenko et al. 2014b)) and in the presence of PEG-4000 (squares) at low (80 mg/L *A*), medium (150 mg/mL, *B*) and high (300 mg/L *C*) concentration. The protein conformational changes were followed by the changes in the parameter *A* (λ_{ex}=297 nm), fluorescence anisotropy *r* at the emission wavelength 365 nm (λ_{ex}=297 nm), the ellipticity at 222 nm and the ANS fluorescence intensity at λ_{em}=480 nm (l_{ex}=365 nm). Protein was incubated in a solution with the appropriate GdnHCl concentration at 4ºC for 1 h (gray squares), 24 h (light green squares and red circles) and 72 h (green squares). The open symbols indicate unfolding, whereas the closed symbols represent refolding.

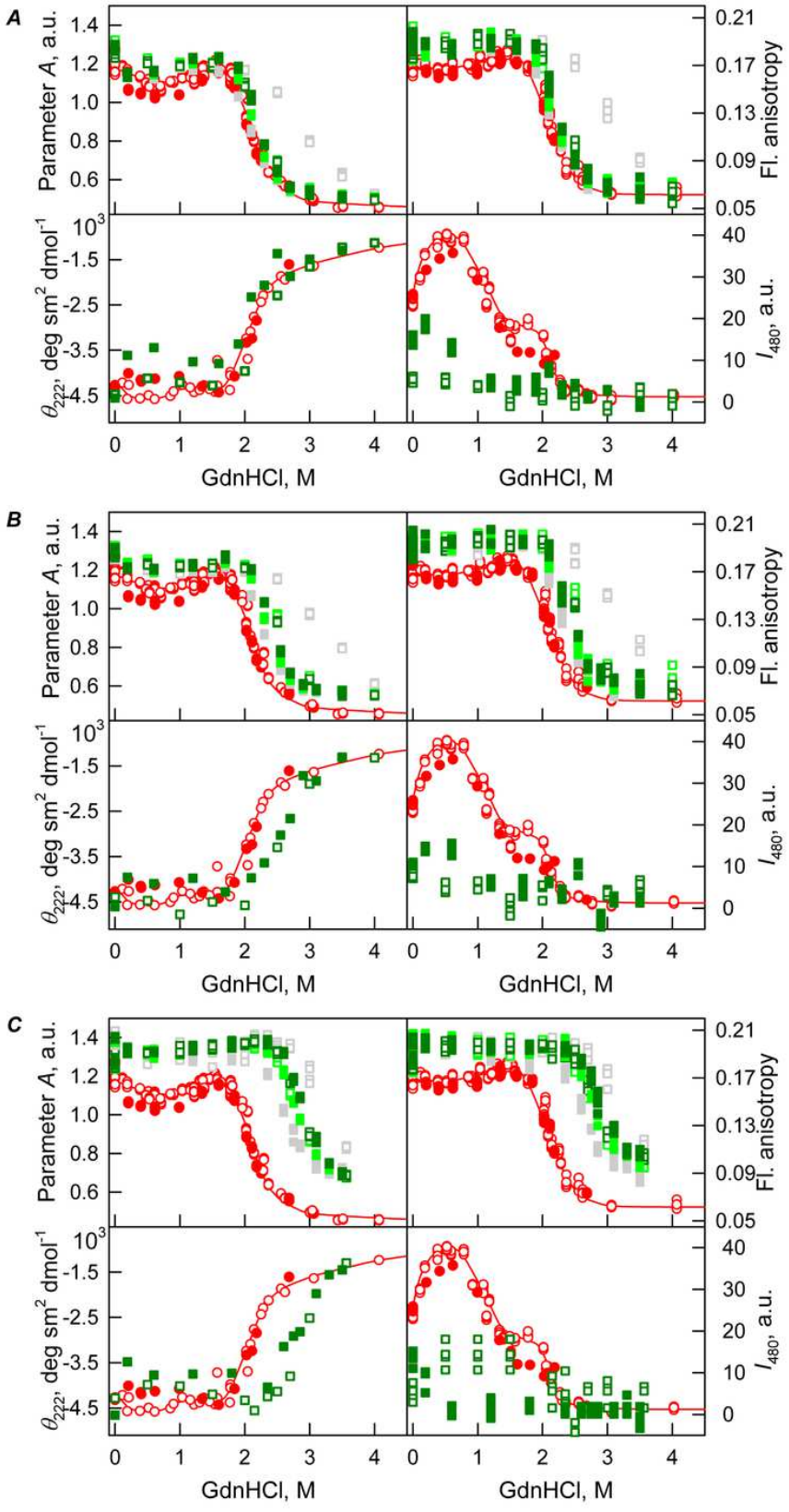

GdnHCl-induced unfolding – refolding of the recombinant bOBP alone and in the presence of PEG-12000 s

Figure 4. GdnHCl-induced unfolding – refolding of the recombinant bOBP alone (red circles; the data are from (Stepanenko et al. 2014b)) and in the presence of PEG-12000 (squares) at low (80 mg/mL, *A*), medium (150 mg/mL, *B*) and high concentrations (300 mg/mL, *C*). The protein conformational changes were followed by changes in the parameter *A* (λ_{ex}=297 nm), fluorescence anisotropy *r* at the emission wavelength 365 nm (λ_{ex}=297 nm), the ellipticity at 222 nm, and the ANS fluorescence intensity at λ_{em}=480 nm (l_{ex}=365 nm). Protein was incubated in a solution with the appropriate GdnHCl concentration at 4ºC for 1 h (gray squares), 24 h (light green squares and red circles) and 72 h (green squares). The open symbols indicate unfolding, whereas the closed symbols represent refolding.

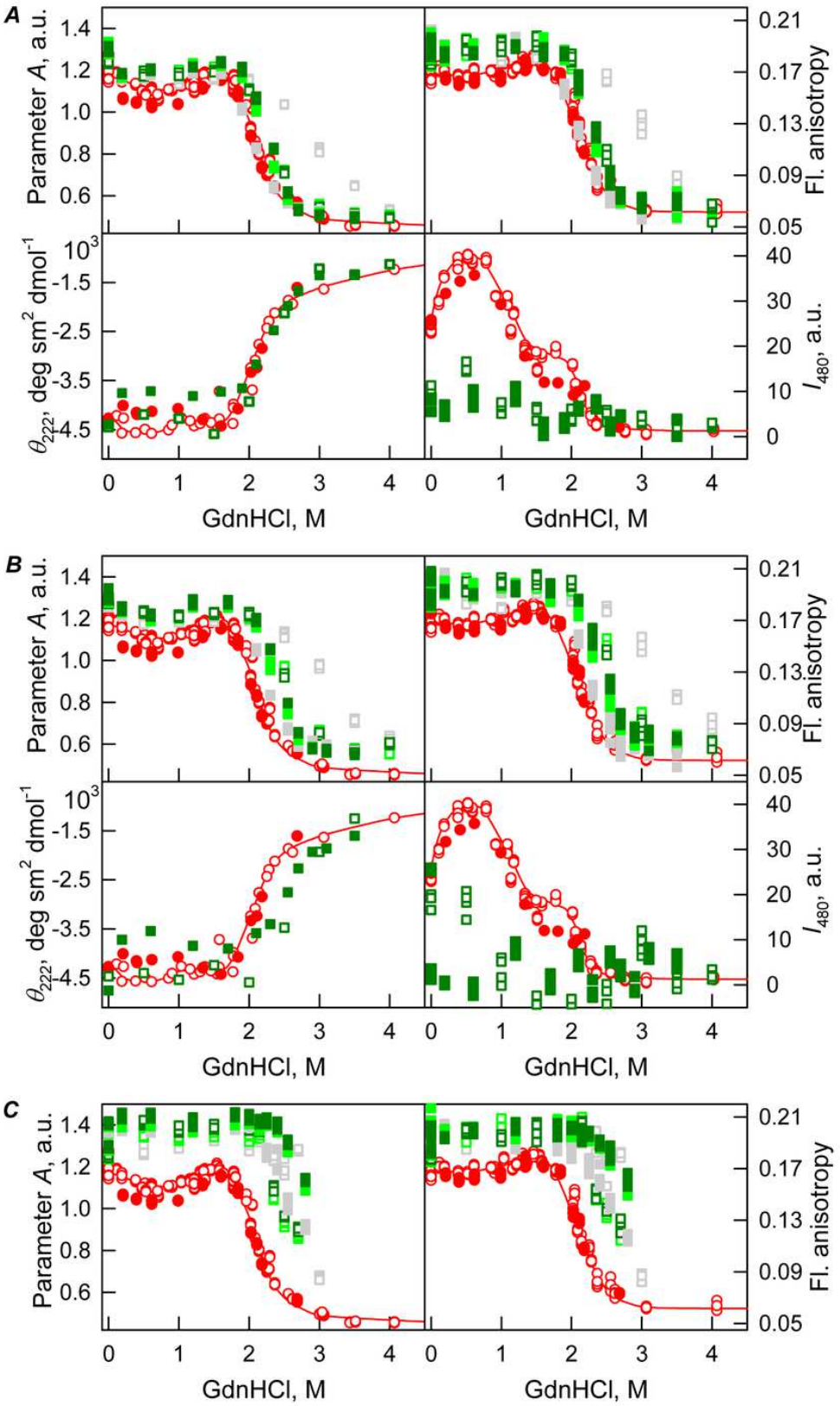

Structural properties of bOBP in crowded environment.

Figure 5. Changes in the near-UV CD spectra (upper panels) and the tryptophan fluorescence spectra (bottom panels) of bOBP alone (black lines) and in the presence of PEG-600 (green colors), PEG-4000 (red colors) and PEG-12000 (blue colors). The measurements were preceded by incubating the protein in a solution with crowding agent at 4ºC for 1 h (PEG-600 – light-green, PEG-4000 – pink, PEG-12000 – light blue) and 72 – 96 h (PEG-600 – green, PEG4-000 – red, PEG-12000 –blue). The concentrations of crowding agents were 80 mg/mL (***A***), 150 mg/mL (***B***) and 300 mg/mL (***C***).

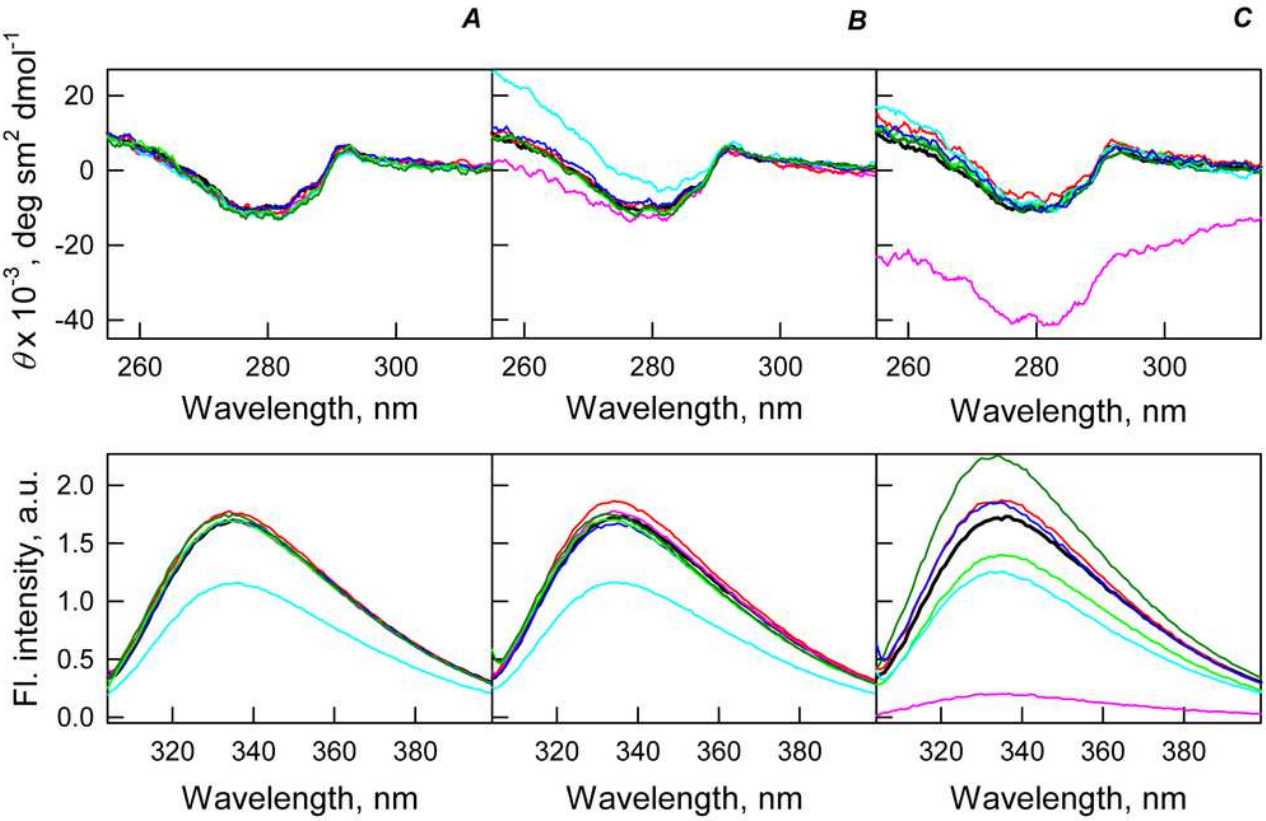

6

GdnHCl-induced unfolding – refolding of the recombinant bOBP alone and in the presence of various crowding agents.

Figure 6. GdnHCl-induced unfolding – refolding of the recombinant bOBP alone (gray circles; the data are from (Stepanenko et al. 2014b)) and in the presence of crowding agents PEG-600 (green colors), PEG-4000 (red colors) and PEG-12000 (blue colors). The protein conformational changes were followed by the changes in parameter *A* and fluorescence anisotropy at the emission wavelength 365 nm (λ_{ex}=297 nm). The measurements were preceded by incubating the protein in a solution with the appropriate GdnHCl concentration at 4ºC for 72 – 96 h. The open symbols indicate unfolding, whereas the closed symbols represent refolding. Applied concentrations of crowding agents were 80 mg/mL (***A***; squares, PEG-600 – light green, PEG-4000 – pink, PEG-12000 – light blue), were 150 mg/mL (***B***; circles, PEG-600 – green, PEG-4000 – red, PEG-12000 –blue) and were 300 mg/mL (***C***; triangles, PEG-600 – dark yellow, PEG-4000 – brown, PEG-12000 – dark blue). ***D*** panel represents all intrinsic fluorescence data for comparison purpose.